Global Maximum Power Point Tracking Method for Photovoltaic Arrays Under Partial Shading Conditions

Alireza Ramyar, Hossein Iman-Eini, *Member, IEEE*, and Shahrokh Farhangi, *Member, IEEE*

***Abstract*—The power–voltage characteristic of photovoltaic (PV) arrays displays multiple local maximum power points when all the modules do not receive uniform solar irradiance, i.e., under partial shading conditions (PSCs). Conventional maximum power point tracking (MPPT) methods are shown to be effective under uniform solar irradiance conditions. However, they may fail to track the global peak under PSCs. This paper proposes a new method for MPPT of PV arrays under both PSCs and uniform conditions. By analyzing the solar irradiance pattern and using the popular Hill Climbing method, the proposed method tracks all local maximum power points. The performance of the proposed method is evaluated through simulations in MATLAB/SIMULINK environment. Besides, the accuracy of the proposed method is proved using experimental results.**

***Index Terms*—Current–voltage (I–V) characteristic, maximum power point tracking (MPPT), partial shading condition (PSC), photovoltaic (PV) array, power–voltage (P–V) characteristic.**

I. Introduction

NOWADAYS, solar energy as a clean and free available renewable energy resource is too important for reducing the dependency on conventional sources. Photovoltaic (PV) systems produce electric power by directly transforming the inexhaustible solar energy into electricity. However, the relatively high cost, low conversion efficiency of electric power generation, dependency on environmental conditions (e.g., solar irradiance and temperature), and nonlinearity of the power–voltage (P–V) and current-voltage (I–V) characteristic of PV arrays are the main challenges in utilization of PV arrays.

Tracking the global peak (GP) of a PV array in all conditions is significantly important to guarantee the maximum achievable power. Many maximum power point tracking (MPPT) methods have been proposed in the literature [1]–[3]. Popular MPPT methods like perturbation and observation (P&O), hill climbing (HC), and incremental conductance (IC) methods are shown to be effective when the solar irradiance condition is uniform for all PV modules. Since, the tracking becomes more complicated under partial shading conditions (PSCs), i.e., when all the modules do not receive uniform solar irradiance, these basic methods fail to track the GP. Though in uniform solar irradiance conditions the P-V characteristic of PV array has just one peak, the P-V characteristic of PV array displays multiple peaks under PSCs. Hence, several MPPT methods are proposed which are applicable in PSCs. These methods can be categorized into two groups: hardware-based methods and software-based methods [4].

In [5] and [6], a controller is assigned for each module. These hardware-based methods can resolve the problem, since the P-V characteristic of a module (with just one bypass diode) always has a single peak. These methods, however, are not cost-effective and require much more devices in comparison to software-based algorithms.

Ishaque *et al.* [7] have proposed an effective MPPT method for PV systems based on particle swarm optimization (PSO) algorithm. This method is too complex to be applied to the commercial appliances, since some parameters have to be set by the user. In [8], artificial neural network (ANN) algorithm has been opted. The main problem of ANN-based methods is that the ANN's accuracy under different conditions is highly dependent to the amount of available training data. In addition, they need to be retrained when the PV array is changed. In [9]–[12] genetic algorithm, flashing fireflies, artificial bee colony, and simulated annealing are used in PV applications, respectively. These methods have good performances but similar to the aforementioned issues for the PSO and ANN methods, the implementation complexity of these methods is their major problem; since they involve complex calculations and several parameters have to be set by user.

In [4], the HC method has been improved. It can efficiently detect the shading condition. Then, by measuring power in suitable points, it chooses the highest one and performs the HC around this point. However, it does not have an acceptable accuracy for tracking the GP, since it compares the power of points near the LPs instead of the LPs themselves. In [13], a modified P&O method has been introduced which benefits from a unique characteristic that has been observed in the P-V curves. Although it has a great performance, since almost two measurements are done for each LP, the tracking speed is low. In [14], it is claimed that the GP is around the intersection of the I-V characteristic of PV arrays and a certain line. It depends on short

Manuscript received July 1, 2016; revised September 20, 2016 and October 9, 2016; accepted October 11, 2016. Date of publication November 24, 2016; date of current version March 8, 2017. This work was supported by the Iran National Science Foundation.

The authors are with the School of Electrical and Computer Engineering, College of Engineering, University of Tehran, Tehran 1439957131, Iran (e-mail: alireza.ramyar@ut.ac.ir; imaneini@ut.ac.ir; farhangi@ut.ac.ir).

Color versions of one or more of the figures in this paper are available online at http://ieeexplore.ieee.org.

Digital Object Identifier 10.1109/TIE.2016.2632679

circuit current of array which is problematic [1]. This problem is almost resolved by updating this value based on the solar irradiance. However, it is uncommon to find sensors that measure solar irradiance levels [1]. In [15], a relationship is defined between the PV power and a control signal to track the P-V curve and find the GP. Although its accuracy is high, it is slow because it searches almost all the range of the P-V curve. The proposed method in [16] uses the critical observations reported in [13] in a different way, but it does not have any procedure for detecting whether there is an LP near the target point or not. As a result, it may fail in some PSCs. Moreover, the approach in [16] involves complex calculations (e.g., calculation of square root) compared to similar methods; hence, it is not as simple as other similar methods for experimental implementation. By choosing lower and upper voltage limits, [17] narrows the searching window and tracks the GP very fast. On the other hand, authors admit that the method may fail when two LPs have nearly equal power values. The proposed method in [18] maps out the solar irradiance pattern based on the voltage of modules and chooses an appropriate voltage to track the GP around it. Obviously, employment of one voltage sensor for each module is not feasible and cost effective. In [19], two methods are proposed. The first one searches the P-V curve for MPPs by means of IC. However, it skips parts of the area based on short circuit current of the modules and the highest local power. This method would be very slow since it must scan almost all the P-V curve. Although the second method has improved the speed of tracking compared to the first one, it still uses one current sensor for each bypass diode, which is not cost effective.

The proposed method in [20] applies ramp voltage command to the converter. Therefore, it avoids the oscillation of voltage and current of the system in transient intervals. Hence, long delays in usual methods for correct sampling of voltage and current are not needed any more. However, it searches almost all the range of P-V curve and therefore, its tracking speed is not good.

Proposing a method which meets accuracy, convergence speed, simplicity, minimum needed parameters, minimum cost, and other important factors [1] at the same time is still of a great importance. In this paper, we propose a novel method for MPPT of PV arrays which works effectively in PSCs and at the same time, has great performance in diverse factors mentioned above. By measuring PV current in defined points, the method maps out the solar irradiance pattern. Based on the mapping, it chooses appropriate points for tracking the LPs. Then, it performs HC in these points and tracks all the LPs. Finally, by comparison of the acquired LPs, it chooses the GP.

II. I-V Characteristic of PV Arrays Under PSCs

A. Single-Diode Model

Based on the single diode model of the PV cells, if N_s modules (each of which consists of $N_{s,m}$ series cells) are serried, and N_p strings are paralleled, the voltage equation of the array would be as follows [21]:

$$V = N_s \left(\frac{akTN_{s,m}}{q}\right) \ln\left[\frac{I_{\text{pv,array}} - I}{I_{0,\text{array}}}\right] - \left(\frac{N_s}{N_p}\right) R_s I \quad (1)$$

where V and I are the output voltage and current of PV array, respectively. $I_{\text{pv,array}}$ is the output current of PV array. $I_{0,\text{array}}$ is the equivalent saturation current. q is the electron charge ($1.60217646 \times 10^{-19}$ C), k is the Boltzman constant ($1.3806503 \times 10^{-23}$ J/K), T is the junction temperature in Kelvin, and a is the diode ideality constant. R_s is the PV module's series resistance.

For $I_{\text{pv,array}}$ and $I_{0,\text{array}}$ we can have [4]

$$I_{\text{pv,array}} = N_p \overbrace{(I_{\text{scn},m} + K_I \Delta T)\frac{G}{G_n}}^{I_{\text{sc},m}} \quad (2)$$

and

$$I_{0,\text{array}} = N_p \frac{(I_{\text{scn},m} + K_I \Delta T)}{\exp\left[\frac{q(V_{\text{ocn},m} + K_V \Delta T)}{akTN_{s,m}}\right] - 1} \quad (3)$$

where $I_{\text{scn},m}$ is the short-circuit current of the module in standard test condition (STC), $I_{\text{sc},m}$ is the short circuit of module in real condition, K_I is the current coefficient, G is the solar irradiance level (W/m^2), and G_n is the nominal solar irradiance level (1000 W/m^2). ΔT is the temperature difference to temperature of STC. $V_{\text{ocn},m}$ is the module open circuit voltage in STC and K_V is the voltage coefficient. Since

$$\exp\left[\frac{q(V_{\text{ocn},m} + K_I \Delta T)}{akTN_{s,m}}\right] >>> 1 \quad (4)$$

(3) can be simplified as

$$I_{0,\text{array}} = N_p \frac{(I_{\text{scn},m} + K_I \Delta T)}{\exp\left[\frac{q(V_{\text{ocn},m} + K_I \Delta T)}{akTN_{s,m}}\right]}. \quad (5)$$

Substituting (2) and (5) into (1) yields

$$V = N_s \left(\frac{akTN_{s,m}}{q}\right) \ln\left[\frac{G}{G_n} - \frac{I}{N_p(I_{\text{scn},m} + K_I \Delta T)}\right] + N_s \overbrace{(V_{\text{ocn},m} + K_V \Delta T)}^{V_{\text{oc},m}} - \left(\frac{N_s}{N_p}\right) R_s I \quad (6)$$

where $V_{\text{oc},m}$ is module's open-circuit voltage in real condition. Having $I_{\text{pv,array}} \approx I_{\text{sc,array}}$ [21], [23], (2) can be rewritten as

$$I_{\text{sc,array}} = N_p \overbrace{(I_{\text{scn},m} + K_I \Delta T) \times \frac{G}{G_n}}^{I_{\text{sc},m}} \quad (7)$$

where $I_{\text{sc,array}}$ is the short circuit current of array.

B. I-V Characteristic of PV Arrays Under PSCs

Fig. 1 shows the I-V characteristic of a sample 3 × 2 array under different PSCs. The modules' parameters are listed in Table I. The modules are modeled based on single diode model in [22] and the equivalent parameters of PV modules are listed in Table II. R_p is the PV module's parallel resistance.

As illustrated in Fig. 1, the value of the current in each step is almost constant up to the end of that step. Keeping this point in mind, by measuring the PV current in specific points and comparing them in a suitable manner which are presented in Section III, the PSC pattern can be mapped. As a result, the

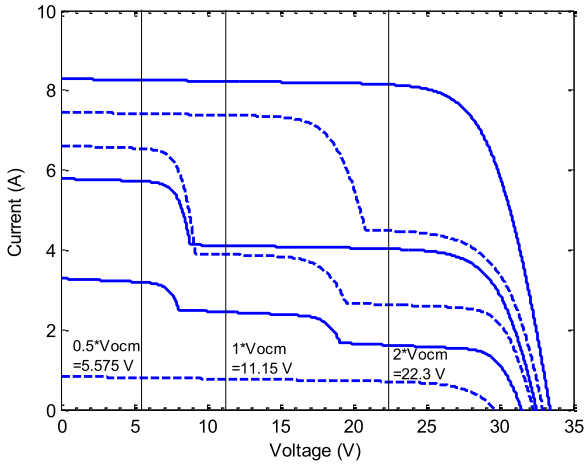

Fig. 1. I-V characteristic of a sample 3 × 2 array under different PSCs when the module open circuit voltage and short circuit current are based on Table I.

TABLE I
PV MODULE'S PARAMETERS

Parameter	VALUE
P_{MPP}	35 W
$V_{oc,n}$	11.15 V
$I_{sc,n}$	4.15 A
$N_{s,m}$	18

TABLE II
EQUIVALENT PARAMETERS OF PV MODULE IN SINGLE DIODE MODEL [22] IN STC

Parameter	VALUE
a	1.077
R_s	0.175 Ω
R_p	123 Ω

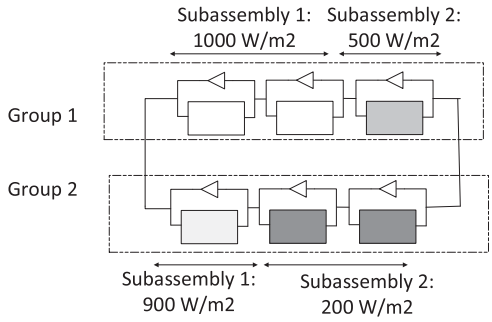

Fig. 2. Sample 3 × 2 PV array under PSC.

number of steps, their lengths, and their order in the I-V characteristic can be detected. In addition, as it is depicted in Fig. 1, voltage values in the starting points of current steps, are in near left-side neighborhood of certain integer multiples of $V_{oc,m}$. In order to justify above claim, a sample PV array consists of two strings each of which includes three series modules, is considered as shown in Fig. 2. The modules' parameters are given in

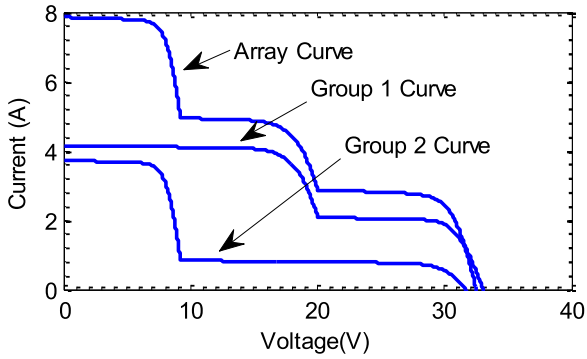

Fig. 3. I-V characteristic of group 1, group 2, and total array in Fig. 2.

Tables I and II. Since the test is executed under STC, ΔT equals to zero and $V_{oc,m}$ equals to $V_{ocn,m}$ which is 11.15 V. Also, Fig. 3 demonstrates the I-V characteristic of each group as well as the total characteristic of the PV array.

1) Group 1 Analysis: The value of the voltage in the starting point of the second step of group 1 can be derived from the voltage of subassembly 1 and 2 in this point:

$$V_{\text{beginning},St2G1} = V_{\text{Sub1}G1} + V_{\text{Sub2}G1} \tag{8}$$

where $V_{\text{beginning},St2G1}$ stands for the voltage of the starting point of the second step in group 1. $V_{\text{Sub1}G1}$ and $V_{\text{Sub2}G1}$ are the voltages of subassembly 1 and 2 in this point, respectively. It should be noticed that in this point, the bypass diode of the module in subassembly 2 is still ON and is going to be OFF. Therefore, the voltage of subassembly 2 in this point derives from the bypass diode's forward voltage, which is 0.8 V in this test

$$V_{\text{Sub2}G1} = -0.8 \text{ V}. \tag{9}$$

Using (7), the short circuit current of the subassembly 2 can be determined as the following equation. In this case $G = 500$, $\Delta T = 0$, and $N_p = 1$

$$I_{\text{sc,Sub2G1}} = 2.075 \text{ A} \tag{10}$$

where $I_{\text{sc,Sub2G1}}$ stands for open-circuit voltage of the subassembly 1 of group 1. Using (6), the corresponding voltage of the subassembly 1 in the start point of the second step can be calculated. In this case $G = 1000$, $\Delta T = 0$, $T = 298.15$ K, $N_s = 2$, $N_p = 1$, and $V_{\text{ocn},m} = 11.15$ V. Also, the value of I in (6) equals to 2.075 A, since the starting point of the second step is the end of the first step. Therefore, one can write

$$V_{\text{Sub1}G1} = 20.883 \text{ V}. \tag{11}$$

Substituting (9) and (11) into (8) yields

$$V_{\text{beginning},St2G1} = 20.083 \text{ V}. \tag{12}$$

As it was claimed, the starting point of the second step (20.083 V) is in near left side neighborhood of certain integer multiple of $V_{oc,m}$ which is $2 \times V_{oc,m}$ (22.3 V) in this case.

2) Group 2 Analysis: The analysis of this group is similar to analysis of group 1. So, the value of the voltage in starting point of the second step of group 2 can be derived from the

voltage of subassembly 1 and 2 in this point

$$V_{\text{beginning},St2G2} = V_{\text{Sub1}G2} + V_{\text{Sub2}G2} \tag{13}$$

where $V_{\text{beginning},St2G2}$ stands for the voltage of the starting point of the second step in group 2. V_{S1G2} and V_{S2G2} are the voltages of subassembly 1 and 2 in this point, respectively. In this point the bypass diodes of the modules in subassembly 2 are still ON and are going to be OFF. Then, the voltage of subassembly 2 in this point derives from the bypass diode's forward voltage, which is 0.8 V in this test

$$V_{\text{Sub}2G2} = -1.6 \text{ V}. \tag{14}$$

The short circuit of the subassembly 2 can be calculated using (7). In this case $G = 200$, $\Delta T = 0$, and $N_p = 1$

$$I_{\text{sc,Sub}2G2} = 0.83\ A \tag{15}$$

where $I_{\text{sc,Sub}2G2}$ stands for open-circuit voltage of the subassembly 1 of group 2. Again by usage of (6), the corresponding voltage of the subassembly 1 in the starting point of the second step can be calculated. In this case $G = 900$, $\Delta T = 0$, $T = 298.15\,\text{K}$, $N_s = 1$, $N_p = 1$, and $V_{\text{ocn},m} = 11.15$ V. Also, the value of I in (6) equals to 0.83 A. Therefore,

$$V_{\text{Sub}1G2} = 10.827 \text{ V}. \tag{16}$$

Substituting (14) and (16) into (13) yields

$$V_{\text{beginning},St2G2} = 9.227 \text{ V}. \tag{17}$$

Similar to group 1, the starting point of the second step (9.227 V) in group 2 is in near left side neighborhood of certain integer multiple of $V_{\text{oc},m}$ which is $1 \times V_{\text{oc},m}$ (11.15 V) in this case.

3) Array Analysis: Since the curves of each group consist of steps in which the values of current are almost constant until the next step, the summation value would also have this characteristic. On the other hand, since the starting points of the total curve are the starting points of the steps in groups 1 and 2, the value of the voltage for each start point is in near left side neighborhood of a certain multiple of $V_{\text{oc},m}$. The proposed analysis is valid for every structure.

III. Proposed Method for MPPT

Fig. 4 shows the flowchart of the proposed method. In steady state conditions, the HC method performs around the last GP which has been detected by the proposed method.

A. Detecting the Solar Irradiance Changes

In order to recognize the sudden changes of the solar irradiance condition, the power difference between each two consecutive cycles *(ΔP)* is calculated and compared against a certain critical power variation (ΔP_{crit}), as illustrated in Fig. 4. If ΔP is higher than ΔP_{crit}, variation of the solar irradiance condition is detected and the global MPPT starts. Generally, the sudden changes in solar irradiance are small in magnitude (smaller than 27 W/m^2) [13]. So, ΔP_{crit} can be equal to the change in output power of array, for the condition that the solar irradiance

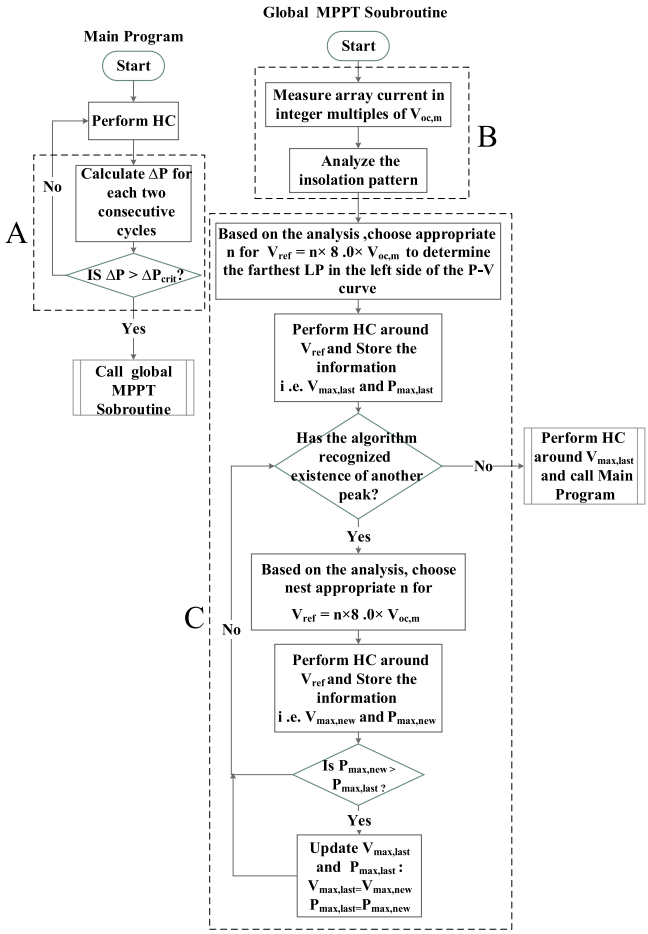

Fig. 4. Flowchart of the proposed method.

changes by 27 W/m^2 [13]. Or, it might be set to an appropriate percentage of array nominal power [13]. In this paper, this threshold is set to 5% of the nominal power, based on trial and error observation from simulation. Once the solar irradiance change is detected, the sections B and C in Fig. 4 start to track the new GP as explained in the following.

B. Analysis of the Solar Irradiance Pattern

In Section B, the method measures the current in the multiples of $V_{\text{oc},m}$. It was proved in Section II-B that the starting point of the current steps in the I-V characteristic are in the near left side neighborhood of certain integer multiples of $V_{\text{oc},m}$. In addition, the value of the current for each step is nearly constant up to the next step. Therefore, by comparing the measured currents against each other, the number of steps, their lengths, and their order in the I-V characteristic can be easily determined by the following procedure.

If I_{Vk} is the measured current in $K \times V_{\text{oc},m}$ and $I_{V(k-1)}$ is the measured current in $(K-1) \times V_{\text{oc},m}$, the proposed method checks the validity of the following inequality:

$$\frac{I_{V(k-1)} - I_{\text{Vk}}}{I_{V(k-1)}} \leq \Delta I_{\text{crit}}. \tag{18}$$

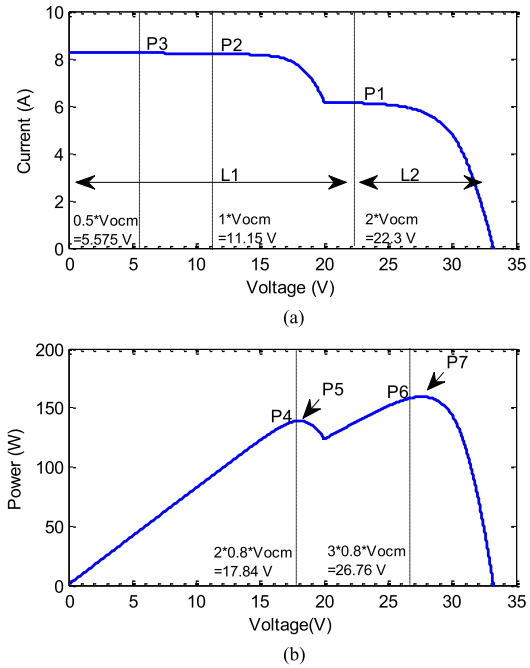

Fig. 5. (a) I-V characteristic and (b) P-V characteristic of a sample 5×5 array.

If this inequality is satisfied, the proposed method recognizes that there is no new step in the neighborhood of $K \times V_{\mathrm{oc},m}$; otherwise the new step is detected by the method. It should be noticed that if the steps were ideal, i.e., the I-V characteristic was constructed from rectangular sections, ΔI_{crit} must be zero. However, the steps are not ideal. Since the current source part of the I-V characteristic of the PV array under uniform conditions continues to maximum power point (in which current is about $0.9 \times I_{\mathrm{sc}}$ [13], [20]), an appropriate value for ΔI_{crit} is $(I_{\mathrm{sc}} - 0.9 \times I_{\mathrm{sc}})/I_{\mathrm{sc}}$ which equals to 0.1. Generally, lower values of ΔI_{crit} lead to higher accuracy, but it increases the time required to track the GP. Since the boost converter is used, it is better to keep distance from zero-voltage point and measure the current of $0.5 \times V_{\mathrm{oc},m}$ instead of the current of zero voltage point. However, measuring the current in a small voltage makes the boost converter to work in a relatively large duty cycle and it is a drawback.

It is helpful to describe this procedure in a sample case. The corresponding I-V and P-V curves of a 3×2 PV array whose parameters are listed in Tables I and II, under a sample PSC are shown in Fig. 5(a) and (b), respectively. For analyzing the PSC pattern, the current of PV array is measured in three points ($2 \times V_{\mathrm{oc},m}$, $1 \times V_{\mathrm{oc},m}$, and $0.5 \times V_{\mathrm{oc},m}$). As it is depicted in Fig. 5(a), these three points are $P_1(22.3\,\mathrm{V}, 6.13\,\mathrm{A})$, $P_2(11.15\,\mathrm{V}, 8.2\,\mathrm{A})$, and $P_3(5.575\,\mathrm{V}, 8.24\,\mathrm{A})$, respectively.

(18) is checked for corresponding currents as follows:

$$\frac{8.24 - 8.2}{8.24} = 0.005 \leq 0.1 \tag{19}$$

$$\frac{8.2 - 6.13}{8.2} = 0.25 > 0.1. \tag{20}$$

Hence, based on the described procedure, the algorithm recognizes that there are two steps in the I-V curve, with the lengths of L_1 $(2 \times V_{\mathrm{oc},m})$ and L_2 $(1 \times V_{\mathrm{oc},m})$. Actually, (18) is true in the case that $k = 1$ which means that P_3 and P_2 are in the same step. Since (18) is not satisfied in the case that $K = 2$, it means that P_1 and P_2 are not in the same steps. Thus, as it was claimed, the proposed method detects the number of steps, their lengths, and their order in the I-V characteristic with just measuring the array current. This new idea is very simple and yet so useful for MPPT in PSCs. It should be mentioned that, although methods like [18] use one voltage sensor for each module to map out the PSC pattern, the new method maps out the PSC pattern with just one current sensor.

C. Searching for Maximum Power Points

Based on [13], the LPs are in neighborhood of integer multiples of $0.8 \times V_{\mathrm{oc},m}$. So according to the analyzed solar irradiance pattern, the method allocates a certain multiple of $0.8 \times V_{\mathrm{oc},m}$, to each LP. Thus by operation of the HC method in its neighborhood, the corresponding LP is tracked. Finally, by comparison among the LPs, the GP is determined.

Whether each LP is tracked or not is recognized by checking the slope of the P-V curve. After determining the largest LP as the GP, the HC is performed around it. When the GP is tracked, the duty cycle is fixed to prevent the perturbations, as discussed in [15]. However, it is not necessarily an issue for the proposed method. Besides, a variable step HC can be used to decrease the perturbations around the GP.

To better understand the above procedure, the previous example is considered for finding the GP. After obtaining the PSC pattern, the HC is performed around P_4(17.84 V) in which voltage equals to $L_1 \times 0.8 \times V_{\mathrm{oc},m}(2 \times 0.8 \times V_{\mathrm{oc},m})$, and tracks $P_5(138.9\,\mathrm{W})$, as it is illustrated in Fig. 5(b). Then, based on the obtained PSC pattern, the algorithm goes to the neighborhoods of the other LP, i.e., $P_6(26.76\,\mathrm{V})$ in which voltage equals to $(L_1 + L_2) \times 0.8 \times V_{\mathrm{oc},m}(3 \times 0.8 \times V_{\mathrm{oc},m})$. The HC method is performed around this point and the other LPs are tracked, which are $P_7(720\,\mathrm{W})$. Finally, by comparison among these LPs, the GP which is $P_6\,(159.3\,\mathrm{W})$ is determined.

Since the proposed method is a search-based tracking algorithm and just initiates the HC method in the neighborhood of $0.8 \times V_{\mathrm{oc},m}$, it does not really depend on the open circuit voltage. But the voltage can be updated every 10 min by the following equation [4]:

$$V_{\mathrm{oc},m} = V_{\mathrm{ocn},m} + K_V \Delta T \tag{21}$$

and after each update, the proposed method can be performed.

As described, the proposed algorithm has modified the conventional HC method to work properly in PSCs. Therefore, it is simple for experimental implementation. Also, as presented in subsequent sections, the accuracy and convergence speed of the proposed method are better than existing methods.

TABLE III
SYSTEM'S PARAMETERS

Parameter	VALUE
L	0.6 mH
C_{in}	34 μF
C_{out}	48 μF
Switching frequency	40 KHz
Sampling frequency	1 KHz
Array nominal open circuit voltage	33.45 V
Array nominal short circuit current	8.3 A
Array nominal power	210 W

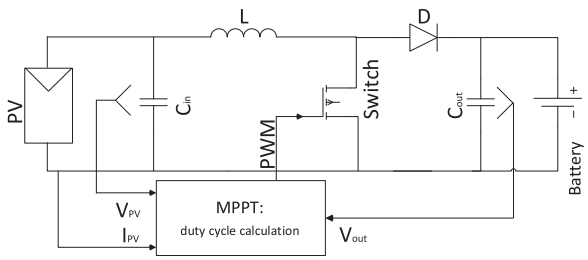

Fig. 6. Schematic of the system.

IV. SIMULATION RESULTS

In this section several simulation results will be presented. The simulated PV system is a 3 × 2 PV array, whose parameters are listed in Tables I and II.

The PV array is connected to a boost DC-DC converter which tracks the maximum power point. There are three series connected 12-V batteries in the output side. The parameters of system under study are listed in Table III. Also the schematic of the system is shown in Fig. 6.

During adoption of HC method, the duty cycle of the boost converter is calculated directly based on the last duty cycle as follows:

$$D_k = D_{k-1} + d_k \tag{22}$$

where D_k and D_{k-1} are the calculated duty cycles in previous [i.e., (K-1)th] and present (i.e., Kth) cycles, respectively. d_k is a number which it's value is constant, but it's sign may change in each cycle. If the value of the power measured in the Kth cycle is larger than the value of power measured in (K-1)th cycle, d_k is calculated as

$$d_k = d_{k-1}. \tag{23}$$

On the other hand, if the power in the Kth cycle is smaller than the power in (K-1)th cycle, d_k is calculated as

$$d_k = -d_{k-1}. \tag{24}$$

Also, when a reference voltage (V_{ref}) is chosen in global MPPT subroutine, the duty cycle (D^*) is generated as follows [13]:

$$D^* = 1 - \frac{V_{\text{ref}}}{V_{\text{out}}}. \tag{25}$$

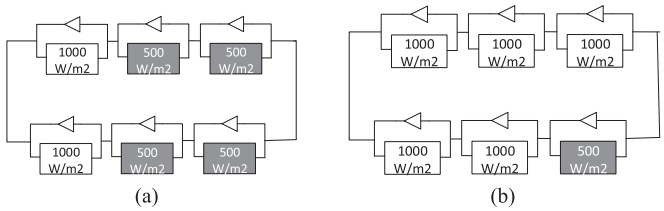

Fig. 7. PSC patterns in the first simulation, (a) from 0.3 to 0.6 s and (b) from 0.6 to 0.9 s.

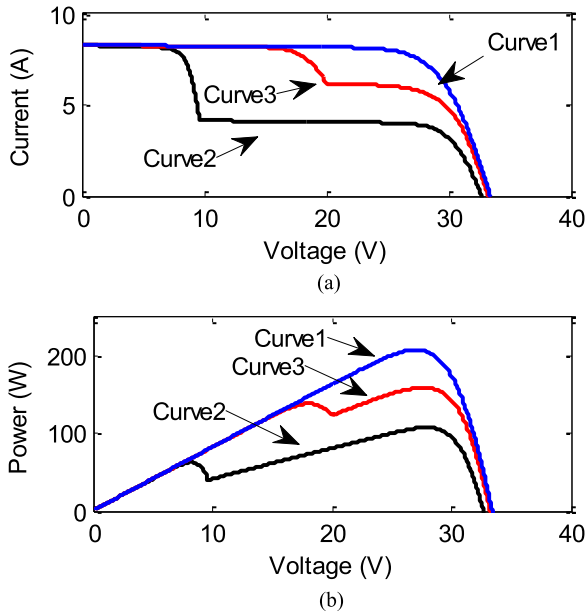

Fig. 8. Corresponding (a) I-V and (b) P-V characteristics under first simulation.

A. Performance Exploration Under Four Consecutive Solar Irradiance Condition

In this section, the performance of the algorithm is tested under four consecutive solar irradiance conditions. From 0 to 0.3 s, the solar irradiance level is equal to 1000 W/m^2 for all the modules. From 0.3 to 0.6 s and 0.6 to 0.9 s, the solar irradiances are shown in Fig. 7(a) and (b), respectively. Finally, from 0.9 to 1.2 s the solar irradiance is equal to 1000 W/m^2 for all the modules again. The I-V and P-V curves of the PV array in these four states are shown in Fig. 8. Array's corresponding voltage, current, power and duty cycle waveforms are shown in Fig. 9(a)–(d), respectively. Moreover, zoomed view of per unit array's voltage, current, power, and duty cycle waveforms in 0.3 to 0.5 s, 0.6 to 0.8 s, and 0.9 to 1.1 s intervals are depicted in Fig. 10(a)–(c), respectively.

As illustrated in Fig. 9(c), the algorithm operates properly under normal conditions and the GP is equal to 208 W which is so close to the peak of curve 1 in Fig. 8(b). It is illustrated in Fig. 10(a) that when the solar irradiance level changes at 0.3 s, the proposed method measures current in $2 \times V_{\text{oc},m}$, $1 \times V_{\text{oc},m}$, and $0.5 \times V_{\text{oc},m}$. Since first and second measured currents are very close and the third differs from these currents, the method recognizes that there are two LPs near $1 \times 0.8 \times V_{\text{oc},m}$ and $3 \times 0.8 \times V_{\text{oc},m}$. The algorithm performs HC and tracks

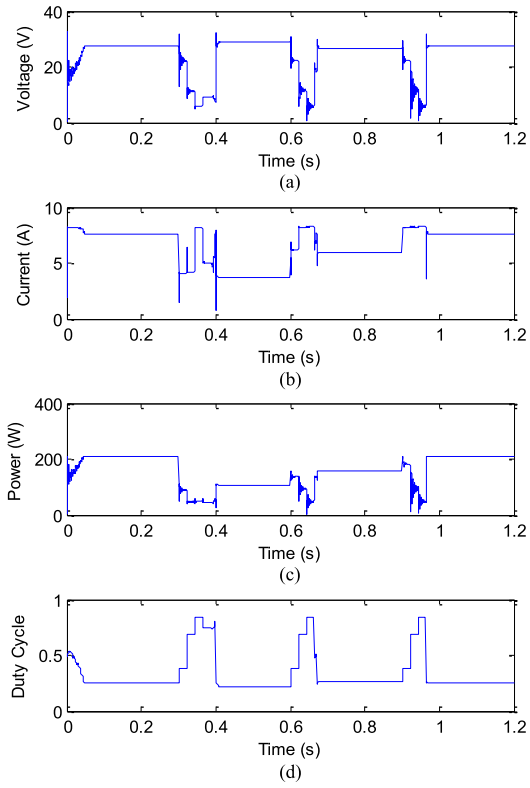

Fig. 9. Corresponding array's (a) voltage, (b) current, (c) power, and (d) duty cycle waveforms in the first simulation.

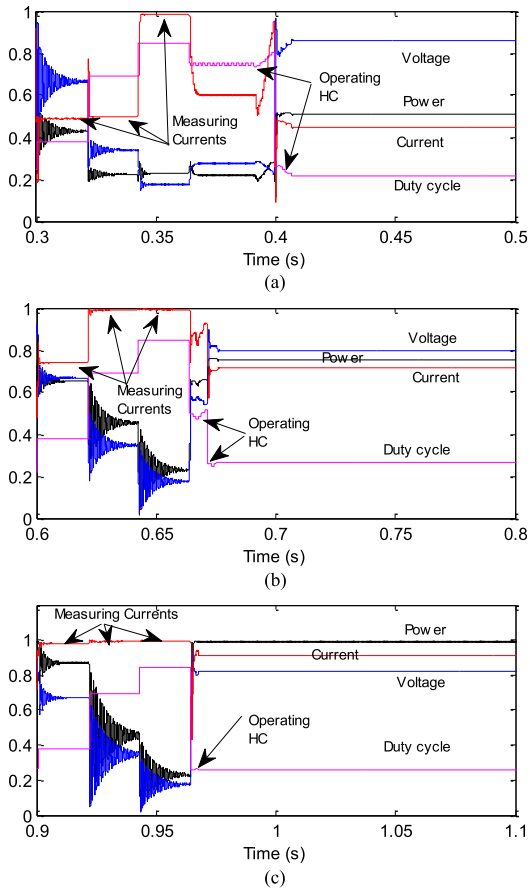

Fig. 10. Zoomed view of per unit array's voltage, current, power, and duty cycle waveforms in the first simulation during (a) 0.3–0.5 s, (b) 0.6–0.8 s, and (c) 0.9–1.1 s intervals. Power should be multiply to 35 × 6, voltage should be multiplied to 3 × 11.15 and current should be multiplied to 2 × 4.15.

two LPs with 59.5 and 107 W power which are very close to the peaks of curve 2 in Fig. 8(b), i.e., 63 and 108 W. So the proposed method chooses the biggest LP and continues to work around 107 W.

Fig. 10(b) shows that when the solar irradiance changes again at 0.6 s, the proposed method starts to measures current in $2 \times V_{oc,m}$, $1 \times V_{oc,m}$, and $0.5 \times V_{oc,m}$. In this case, second and third measured currents are very close and the first one differs from these currents. Thus, the method recognizes that there are two LPs near $2 \times 0.8 \times V_{oc,m}$ and $3 \times 0.8 \times V_{oc,m}$. The algorithm performs HC and tracks two LPs with 139 and 158 W power which are very close to the peaks of curve 3 in Fig. 8(b), i.e., 139 and 159 W. Therefore, the proposed method chooses the biggest LP and continues to work around 159 W.

As it is shown in Fig. 10(c), when the PSC is removed at 0.9 s, the proposed method starts to measures the current in $2 \times V_{oc,m}$, $1 \times V_{oc,m}$, and $0.5 \times V_{oc,m}$. In this case, all measured currents are very close. Hence, the method recognizes that there is just one LP near $3 \times 0.8 \times V_{oc,m}$. The algorithm operates HC and tracks the LP with 208 W power which is very close to the peak of curve 1 in Fig. 8(b). So the proposed method continues to work around 208 W.

B. Comparison of the New Method Against Other Methods

As it was mentioned before, although a large amount of studies are presented in this field, proposing a method which meets accuracy, convergence speed, simplicity, minimum needed parameters, and other important factors is still of a great importance. In this section, simulations are done to compare the new method against two highly cited methods to show its benefits over those. It should be considered that prior works, such as [23], has shown that some of main hypothesis in [13] are not correct, and it may fail to track the GP in some conditions. However, still [13] is now a classic and highly cited method, and most algorithms are compared to it. For comparing the proposed method against [13] and [17], a PSC pattern depicted in Fig. 11(a) is applied to the PV array. The corresponding P-V curve is shown in Fig. 11(b). Also, the corresponding power waveforms of the proposed method, [13] and [17] are illustrated in Fig. 12(a)–(c), respectively.

It is illustrated in Fig. 12(a) that the proposed method tracks the GP with corresponding 97 W power within 0.093 s. The method proposed in [13] tracks the same peak [i.e., the GP in Fig. 11(b) with 99 W power], but in a longer time which is 0.103 s.

Although the method in [17] is faster than two other methods and tracks the peak within 0.077 s, it fails to track the GP correctly. It tracks the middle LP in the P-V curve (87.5 W) instead of the GP. So, it is proved that the proposed method in

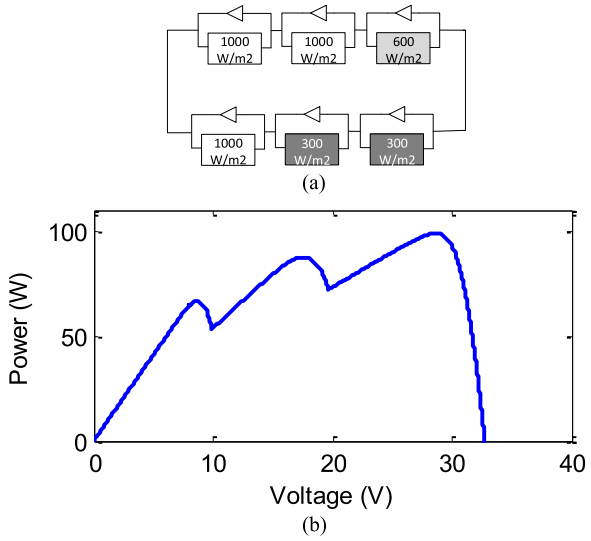

Fig. 11. Corresponding (a) PSC pattern and (b) P-V characteristics under second simulation.

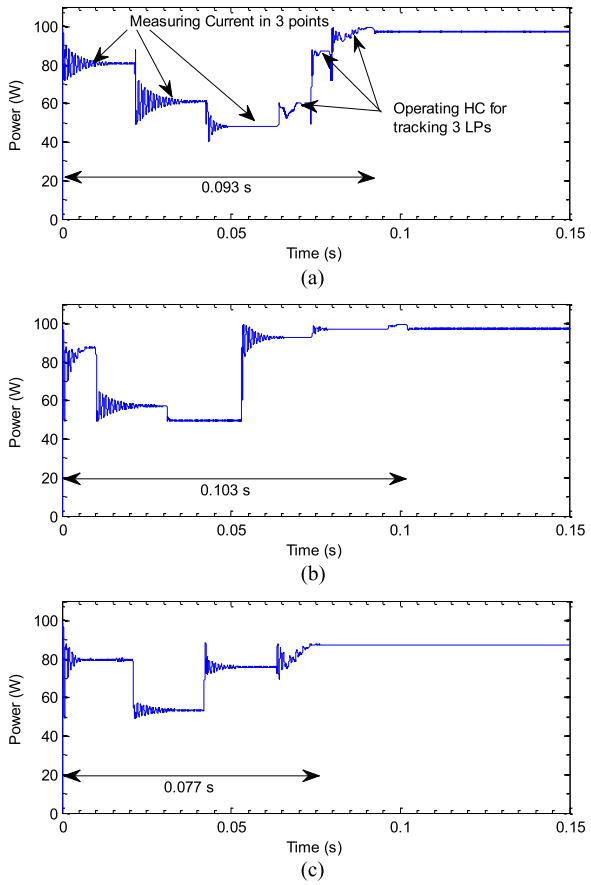

Fig. 12. Comparison of the performance of (a) the proposed method, (b) the proposed method in [13], and (c) the proposed method in [17].

this paper has good performance in both speed and accuracy factors in comparison to two highly cited methods.

Table IV summarizes the comparison of three methods in important factors such as accuracy, convergence speed, implementation complexity, and needed parameters. As demonstrated in Table IV, the proposed method has an appropriate relative performance in comparison to other two highly cited methods.

TABLE IV
COMPARISON OF THREE METHODS IN IMPORTANT FACTORS

	ACCURACY	CONVERGENCE SPEED	IMPLEMENTATION COMPLEXITY	NEEDED PARAMETERS
New method	Very high	High	Low	$V_{oc,m}$ and $N_{s,m}$
[13]	Medium	Medium	Low	$V_{oc,m}$ and $V_{oc,array}$
[17]	High	Very high	Low	$V_{oc,m}$, $I_{sc,array}$ and $V_{oc,array}$ in STC

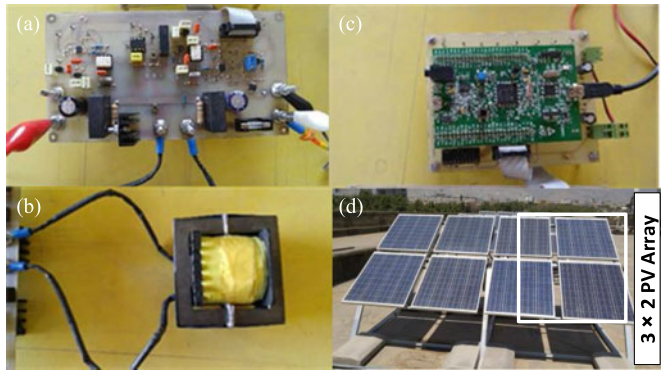

Fig. 13. Experimental setup: (a) the boost converter, (b) converter's inductor, (c) STM32F4 Discovery kit with ARM Cortex-M4 32-bit core on the interface board, and (d) PV array.

TABLE V
ELEMENTS OF EXPERIMENTAL SETUP

Element	NAME
ARM processor	STM32F4 Discovery kit with ARM Cortex-M4 32-bit core
MOSFET switch	IRFP260N
Diode	BYW80-200
Current sensor	ACS 712
Voltage sensor	HCPL 7840

V. EXPERIMENTAL RESULTS

In order to check the validity of the proposed method in practice, the PV modules whose parameters are listed in Tables I and II are used. The configuration of the array (i.e., 3 × 2 array), the schematic of the system, and the parameters of setup under study are similar to the simulation one. In addition, the boost converter, interface board, and PV array are depicted in Fig. 13. The elements used in the experimental setup are listed in Table V. The shadows are applied via dark laminates in experimental tests manually.

In order to compare the proposed method to the methods of [13] and [17], a test with a PSC similar to the PSC in the second simulation is done. By changing the duty cycle gradually, the voltage has changed from 2 V to about 30 V and the corresponding power and current are derived. The corresponding voltage, power, and current of array are illustrated in Fig. 14(a). As it

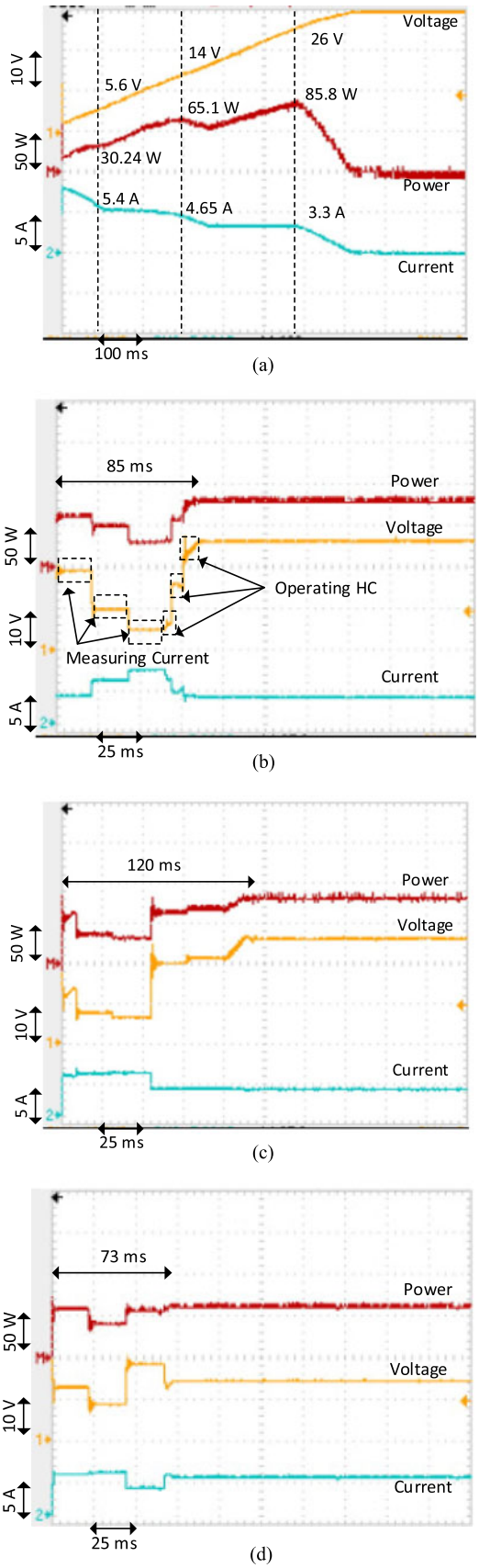

Fig. 14. (a) Corresponding array power, voltage, and current in experimental test, performance of (b) the proposed method, (c) [13], and (d) [17].

TABLE VI
COMPARISON OF THE NEW METHOD WITH PROPOSED METHODS IN [13] AND [17]

	Method	Tracked power (W)	Tracking time (s)	Tracking efficiency (%)	Achievable power (W)
Experimental investigation	New method	83	0.085	97	85.8
	[13]	82	0.12	97	
	[17]	63	0.073	73	
Simulation investigation	New method	97	0.093	98	99
	[13]	97	0.103	98	
	[17]	87.5	0.077	88	

is shown, three LPs which are (5.6 V, 5.4 A, 30.24 W), (14 V, 4.65 A, 65.1 W), and (26 V, 3.3 A, 85.8 W) exist and the last one is the GP. Fig. 14(b)–(d) shows the performance of the proposed method, [13], and [17] in this condition, respectively. It can be seen that the proposed method tracks the GP with 83 W power within 0.085 s. The method proposed in [13] tracks the same peak with 82 W power, but in a longer time which is 0.12 s.

Similar to the second simulation, the method in [17] is faster than two other methods and tracks the peak within 0.073 s, but it fails to track the GP correctly. It tracks the middle LP in the P-V curve with 63 W power instead of the GP.

So, as it was proved in the second simulation, the experimental results show that the proposed method in this paper outperforms the two other methods in both speed and accuracy. The performances of these three methods in the second simulation test and experimental test are summarized in Table VI.

VI. Conclusion

In this paper, a novel MPPT method was proposed which has a great performance under PSC. Based on the simulation and experimental results, it was shown that the current in each step of the I-V characteristic is almost constant until the beginning point of the next step. In addition, it was proved that the starting points of each step in the I-V curve are in near left side neighborhood of the multiples of $V_{oc,m}$.

The proposed method is in fact, a modified HC method which tracks the GP effectively under different conditions. Thus, the implementation of this method is simple. Once the PSCs appear, the number and length of I-V characteristic's steps are recognized by measuring the current value in multiples of $V_{oc,m}$. Then, around specific multiples of $0.8 \times V_{oc,m}$ the HC method tracks all LPs. Finally, the GP is detected by comparing the LPs. Simulation and experimental results have validated the advantages of this method in terms of accuracy and speed over two popular existing methods.

References

[1] T. Esram and P. L. Chapman, "Comparison of photovoltaic array maximum power point tracking techniques," *IEEE Trans. Energy Convers.*, vol. 22, no. 2, pp. 439–449, Jun. 2007.

[2] K. Ishaque and Z. Salam, "A review of maximum power point tracking techniques of PV system for uniform insolation and partial shading condition," *Renew. Sustain. Energy Rev.*, vol. 19, pp. 475–488, Mar. 2013.

[3] L. Liqun, X. Meng, and C. Liu. "A review of maximum power point tracking methods of PV power system at uniform and partial shading," *Renew. Sustain. Energy Rev.*, vol. 53, pp. 1500–1507, Jan. 2016.
[4] A. Kouchaki, H. Iman-Eini, and B. Asaei, "A new maximum power point tracking strategy for PV arrays under uniform and non-uniform insolation conditions," *Solar Energy*, vol. 91, pp. 221–232, May 2013.
[5] R. C. Pilawa-Podgurski and D. J. Perreault, "Submodule integrated distributed maximum power point tracking for solar photovoltaic applications," *IEEE Trans. Power Electron.*, vol. 28, no. 6, pp. 2957–2967, Jun. 2013.
[6] C. Woei-Luen and C. Tsai. "Optimal balancing control for tracking theoretical global MPP of series PV modules subject to partial shading." *IEEE Trans. Ind. Electron.*, vol. 62, no. 8, pp. 4837–4848, Aug. 2015.
[7] K. Ishaque, Z. Salam, M. Amjad, and S. Mekhilef, "An improved Particle Swarm Optimization (PSO)–based MPPT for PV with reduced steady-state oscillation," *IEEE Trans. Power Electron.*, vol. 27, no. 8, pp. 3627–3638, Aug. 2012.
[8] E. Karatepe and T. Hiyama, "Performance enhancement of photovoltaic array through string and central based MPPT system under non-uniform irradiance conditions," *Energy Convers. Manage.*, vol. 62, pp. 131–140, Oct. 2012.
[9] S. Daraban, D. Petreus, and C. Morel, "A novel global MPPT based on genetic algorithms for photovoltaic systems under the influence of partial shading," in *Proc. Annu. Conf. IEEE Ind. Electron. Soc.*, Vienna, Austria, Nov. 2013, pp. 1490–1495.
[10] K. Sundareswaran, S. Peddapati, and S. Palani, "MPPT of PV systems under partial shaded conditions through a colony of flashing fireflies," *IEEE Trans. Energy Convers.*, vol. 29, no. 2, pp. 463–472, Jun. 2014.
[11] K. Sundareswarm, P. Sankar, P. S. R. Nayak, S. P. Simon, and S. Palani, "Enhanced energy output from a PV system under partial shaded conditions through artificial bee colony," *IEEE Trans. Sustain. Energy*, vol. 6, no. 1, pp. 198–209, Jan. 2015.
[12] S. Lyden and M. E. Haque, "A simulated annealing global maximum power point tracking approach for PV modules under partial shading conditions," *IEEE Trans. Power Electron.*, vol. 31, no. 6, pp. 4171–4181, Jun. 2016.
[13] H. Patel and V. Agarwal, "Maximum power point tracking scheme for PV systems operating under partially shaded conditions," *IEEE Trans. Ind. Electron.*, vol. 55, no. 4, pp. 1689–1698, Apr. 2008.
[14] J. Qi, Y. Zhang, and Y. Chen, "Modeling and maximum power point tracking (MPPT) method for PV array under partial shade conditions," *Renew. Energy*, vol. 66, pp. 337–345, Jun. 2014.
[15] E. Koutroulis and F. Blaabjerg, "A new technique for tracking the global maximum power point of PV arrays operating under partial-shading conditions," *IEEE J. Photovolt.*, vol. 2, no. 2, pp. 184–190, Apr. 2012.
[16] KS. Tey and S. Mekhilef, "Modified incremental conductance algorithm for photovoltaic system under partial shading conditions and load variation," *IEEE Trans. Ind. Electron.*, vol. 61, no. 10, pp. 5384–5392, Oct. 2014.
[17] M. Boztepe, F. Guinjoan, G. Velasco-Quesada, S. Silvestre, A. Chouder, and E. Karatepe, "Global MPPT scheme for photovoltaic string inverters based on restricted voltage window search algorithm," *IEEE Trans. Ind. Electron.*, vol. 61, no. 7, pp. 3302–3312, Jul. 2014.
[18] K. Chen, S. Tian, Y. Cheng, and L. Bai, "An improved MPPT controller for photovoltaic system under partial shading condition," *IEEE Trans. Sustain. Energy*, vol. 5, no. 3, pp. 978–985, Jul. 2014.
[19] W. Yunping, Y. Li, and X. Ruan, "High-accuracy and fast-speed MPPT methods for PV string under partially shaded conditions," *IEEE Trans. Ind. Electron.*, vol. 63, no. 1, pp. 235–245, Jan. 2016.
[20] M. A. Ghasemi, H. Mohammadian Forushani, and M. Parniani. "Partial shading detection and smooth maximum power point tracking of PV arrays under PSC," *IEEE Trans. Power Electron.*, vol. 31, no. 9, pp. 6281–6292, Sep. 2016.
[21] P. Lei, Y. Li, and J. E. Seem, "Sequential ESC-Based Global MPPT Control for Photovoltaic Array With Variable Shading," *IEEE Trans. Sustain. Energy*, vol. 2, no. 3, pp. 348–358, Jul. 2011.
[22] M. G. Villalva and J. R. Gazoli, "Comprehensive approach to modeling and simulation of photovoltaic arrays," *IEEE Trans. Power Electron.*, vol. 24, no. 5, pp. 1198–1208, May 2009.
[23] S. Kazmi, H. Goto, O. Ichinokura, and H. J. Guo. "An improved and very efficient MPPT controller for PV systems subjected to rapidly varying atmospheric conditions and partial shading," in *Proc. Australasian Univ. Power Eng. Conf.*, 2009, pp. 1–6.

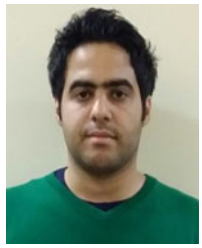

Alireza Ramyar received the B.Sc. degree in electrical engineering from Sharif University of Technology, Tehran, Iran, in 2013, and the M.Sc. degree in electrical engineering from the University of Tehran, Tehran, Iran, in 2015.

He is currently with the Power Electronics and Energy Systems Laboratory, School of Electrical and Computer Engineering, University of Tehran. His research interests include design, modeling and control of power converters, photovoltaics, and renewable energy systems.

Hossein Iman-Eini (M'10) received the B.S. and M.S. degrees from the University of Tehran, Tehran, Iran, in 2001 and 2003, respectively, and the Ph.D. degree jointly from the University of Tehran and the Grenoble Institute of Technology, Grenoble, France, in 2009, all in electrical engineering.

He is currently an Associate Professor in the School of Electrical and Computer Engineering, University of Tehran. His current research interests include the modeling and control of power converters, multilevel converters, and renewable energy systems.

Shahrokh Farhangi (M'90) received the B.Sc., M.Sc., and Ph.D. degrees in electrical engineering, with honors, from the University of Tehran, Tehran, Iran, in 1972, 1973, and 1994, respectively.

He is currently a Professor in the School of Electrical and Computer Engineering, University of Tehran. His research interests include design and modeling of power electronic converters, drives, photovoltaics, and renewable energy systems. He has published more than 100 papers in conference proceedings and journals. He has managed several research and industrial projects, some of which have won national and international awards.

Prof. Farhangi was named as a Distinguished Engineer in Electrical Engineering by the Iran Academy of Sciences in 2008.